

Organic semiconductor distributed feedback (DFB) laser as excitation source in Raman spectroscopy

Xin Liu,^{1,2} Panagiotis Stefanou,¹ Bohui Wang,¹ Thomas Woggon,^{1,2,3} Timo Mappes,^{2,4} and Uli Lemmer^{1,2,*}

¹ Light Technology Institute (LTI) and DFG-Center for Functional Nanostructures (CFN), Karlsruhe Institute of Technology (KIT), 76128 Karlsruhe, Germany

² Institute of Microstructure Technology (IMT), Karlsruhe Institute of Technology (KIT), 76128 Karlsruhe, Germany

³ VISOLAS GmbH, Hermann-von-Helmholtz-Platz 1, 76344 Eggenstein-Leopoldshafen, Germany

⁴ currently with Carl Zeiss AG, Jena, Germany

*uli.lemmer@kit.edu

Abstract: As an application of organic semiconductor distributed feedback (DFB) lasers we demonstrate their use as excitation sources in Raman spectroscopy. We employed an efficient small molecule blend, a high quality resonator and a novel encapsulation method resulting in an improved laser output power, a reduced laser line width and an enhanced power stability. Based on these advances, Raman spectroscopy on selected substances was enabled. Raman spectra of sulfur and cadmium sulfide are presented and compared with the ones excited by a helium-neon laser. We also fabricated a spectrally tunable organic semiconductor DFB laser to optimize the Raman signals for a given optical filter configuration.

©2013 Optical Society of America

OCIS codes: (140.3490) Lasers, distributed-feedback; (140.7300) Visible lasers; (180.5655) Raman microscopy; (300.6450) Spectroscopy, Raman.

References and links

1. C. V. Raman and K. S. Krishnan, "A new type of secondary radiation," *Nature* **121**(3048), 501–502 (1928).
2. G. Landsberg and L. Mandelstam, "Eine neue Erscheinung bei der Lichtzerstreuung in Kristallen," *Naturwissenschaften* **16**(28), 557–558 (1928).
3. J. H. Giles, D. A. Gilmore, and M. B. Denton, "Quantitative analysis using Raman spectroscopy without spectral standardization," *J. Raman Spectrosc.* **30**(9), 767–771 (1999).
4. O. Svensson, M. Josefson, and F. W. Langkilde, "Reaction monitoring using Raman spectroscopy and chemometrics," *Chemom. Intell. Lab. Syst.* **49**(1), 49–66 (1999).
5. A. Yamada, N. Kojima, K. Takahashi, T. Okamoto, and M. Konagai, "Raman study of epitaxial Ga₂Se₃ films grown by molecular beam epitaxy," *Jpn. J. Appl. Phys.* **31**(Part 2, No. 2B), L186–L188 (1992).
6. T. Jawhari, A. Roid, and J. Casado, "Raman spectroscopic characterization of some commercially available carbon black materials," *Carbon* **33**(11), 1561–1565 (1995).
7. S. Nakashima and H. Harima, "Raman investigation of SiC polytypes," *Phys. Status Solidi A.* **162**(1), 39–64 (1997).
8. U. Schmidt, S. Hild, W. Ibach, and O. Hollricher, "Characterization of thin polymer films on the nanometer scale with confocal Raman AFM," *Macromol. Symp.* **230**(1), 133–143 (2005).
9. I. Nabiev, I. Chourpa, and M. Manfait, "Applications of Raman and surface-enhanced Raman scattering spectroscopy in medicine," *J. Raman Spectrosc.* **25**(1), 13–23 (1994).
10. E. E. Lawson, B. W. Barry, A. C. Williams, and H. G. M. Edwards, "Biomedical applications of Raman spectroscopy," *J. Raman Spectrosc.* **28**(2-3), 111–117 (1997).
11. L.-P. Choo-Smith, H. G. M. Edwards, H. P. Endtz, J. M. Kros, F. Heule, H. Barr, J. S. Robinson, Jr., H. A. Bruining, and G. J. Puppels, "Medical applications of Raman spectroscopy: From proof of principle to clinical implementation," *Biopolymers* **67**(1), 1–9 (2002).
12. A. Ramoji, U. Neugebauer, T. Bocklitz, M. Foerster, M. Kiehntopf, M. Bauer, and J. Popp, "Toward a spectroscopic hemogram: Raman spectroscopic differentiation of the two most abundant leukocytes from peripheral blood," *Anal. Chem.* **84**(12), 5335–5342 (2012).
13. F. Adar, R. Geiger, and J. Noonan, "Raman spectroscopy for process/quality control," *Appl. Spectrosc. Rev.* **32**(1-2), 45–101 (1997).
14. J. M. Andrade, S. Garriques, M. De la Guardia, M. Gomez-Carracedo, and D. Prada, "Non-destructive and clean prediction of aviation fuel characteristics through Fourier transform-Raman spectroscopy and multivariate calibration," *Anal. Chim. Acta* **482**(1), 115–128 (2003).

15. G. Abstreiter, E. Bauser, A. Fischer, and K. Ploog, "Raman spectroscopy-A versatile tool for characterization of thin films and heterostructures of GaAs and Al_xGa_{1-x}As," *Appl. Phys. (Berl.)* **16**(4), 345–352 (1978).
16. M. S. Dresselhaus, A. Jorio, M. Hofmann, G. Dresselhaus, and R. Saito, "Perspectives on carbon nanotubes and graphene Raman spectroscopy," *Nano Lett.* **10**(3), 751–758 (2010).
17. J. N. Chen, G. Conache, M. E. Pistol, S. M. Gray, M. T. Borgström, H. Xu, H. Q. Xu, L. Samuelson, and U. Håkanson, "Probing strain in bent semiconductor nanowires with Raman spectroscopy," *Nano Lett.* **10**(4), 1280–1286 (2010).
18. T. H. Maiman, "Stimulated optical radiation in Ruby," *Nature* **187**(4736), 493–494 (1960).
19. I. R. Lewis and H. G. M. Edwards, *Handbook of Raman Spectroscopy: From the Research Laboratory to the Process Line* (CRC, 2001).
20. D. L. Andrews and A. A. Demidov, *An Introduction to Laser Spectroscopy* (Plenum, 1995).
21. F. Hide, M. Diaz-Garcia, B. Schwartz, M. Andersson, and A. Heeger, "Semiconducting polymers: a new class of solid-state laser materials," *Science* **273**(5283), 1833–1836 (1996).
22. I. D. W. Samuel and G. A. Turnbull, "Organic semiconductor lasers," *Chem. Rev.* **107**(4), 1272–1295 (2007).
23. Y. Oki, S. Miyamoto, M. Maeda, and N. J. Vasa, "Multiwavelength distributed-feedback dye laser array and its application to spectroscopy," *Opt. Lett.* **27**(14), 1220–1222 (2002).
24. T. Woggon, S. Klinkhammer, and U. Lemmer, "Compact spectroscopy system based on tunable organic semiconductor lasers," *Appl. Phys. B* **99**(1-2), 47–51 (2010).
25. S. Klinkhammer, T. Woggon, C. Vannahme, T. Mappes, and U. Lemmer, "Optical spectroscopy with organic semiconductor lasers," *Proc. SPIE* **7722**, 77221I (2010).
26. V. Kozlov, V. Bulovic, P. Burrows, M. Baldo, V. Khalfin, G. Parthasarathy, S. Forrest, Y. You, and M. Thompson, "Study of lasing action based on Foerster energy transfer in optically pumped organic semiconductor thin films," *J. Appl. Phys.* **84**(8), 4096–4108 (1998).
27. C. Vannahme, S. Klinkhammer, M. B. Christiansen, A. Kolew, A. Kristensen, U. Lemmer, and T. Mappes, "All-polymer organic semiconductor laser chips: Parallel fabrication and encapsulation," *Opt. Express* **18**(24), 24881–24887 (2010).
28. O. V. Butrimovich, E. S. Voropai, A. P. Lugovskii, Y. L. Ptashnikov, and M. P. Samtsov, "Mechanisms of photodestruction of 4-dicyano-methylene-2-methyl-6-n-dimethylaminostyryl-4-h-pyran under visible-light," *Opt. Spectrosc.* **69**, 343–345 (1990).
29. S. Riechel, U. Lemmer, J. Feldmann, S. Berleb, A. G. Mückl, W. Brütting, A. Gombert, and V. Wittwer, "Very compact tunable solid-state laser utilizing a thin-film organic semiconductor," *Opt. Lett.* **26**(9), 593–595 (2001).
30. E. D. Palik, *Handbook of Optical Constants of Solids II* (Academic, 1991).
31. A. T. Ward, "Raman spectroscopy of sulfur, sulfur-selenium, and sulfur-arsenic mixtures," *J. Phys. Chem.* **72**(12), 4133–4139 (1968).
32. S. N. White, R. M. Dunk, E. T. Peltzer, J. J. Freeman, and P. G. Brewer, "In situ Raman analyses of deep-sea hydrothermal and cold seep systems (Gorda Ridge and Hydrate Ridge)," *Geochem. Geophys. Geosyst.* **7**(5), 1–12 (2006).
33. D. Himmel, L. C. Maurin, O. Gros, and J.-L. Mansot, "Raman microspectrometry sulfur detection and characterization in the marine ectosymbiotic nematode *Eubostrichus diana* (Desmodoridae, Stilbonematidae)," *Biol. Cell* **101**(1), 43–54 (2009).
34. S. N. White, "Laser Raman spectroscopy as a technique for identification of seafloor hydrothermal and cold seep minerals," *Chem. Geol.* **259**(3-4), 240–252 (2009).
35. S. Klinkhammer, T. Woggon, U. Geyer, C. Vannahme, S. Dehm, T. Mappes, and U. Lemmer, "A continuously tunable low-threshold organic semiconductor distributed feedback laser fabricated by rotating shadow mask evaporation," *Appl. Phys. B* **97**(4), 787–791 (2009).
36. C. A. Arguello, D. L. Rousseau, and S. P. S. Porto, "First-order Raman effect in wurtzite-type crystals," *Phys. Rev.* **181**(3), 1351–1363 (1969).
37. M. Abdulkhadar and B. Thomas, *Nanostruct.* "Study of raman spectra of nanoparticles of CdS and ZnS," *Mater.* **5**, 289–298 (1995).
38. F. X. Gu, H. K. Yu, W. Fang, and L. M. Tong, "Low-threshold supercontinuum generation in semiconductor nanoribbons by continuous-wave pumping," *Opt. Express* **20**(8), 8667–8674 (2012).
39. R. T. Downs, (2006) The RRUFF Project: an integrated study of the chemistry, crystallography, Raman and infrared spectroscopy of minerals. Program and Abstracts of the 19th General Meeting of the International Mineralogical Association in Kobe, Japan. O03–13.

1. Introduction

Since the first reports in 1928 [1, 2], Raman spectroscopy has played an increasingly important role in chemometrics [3, 4], material science [5–8], life science [9–12], quality control in industrial processes [13, 14] and recently in nanostructure characterization [15–17]. The advent of laser as an intense and monochromatic source of excitation light improved the Raman signals dramatically [18–20]. Enabled by the broad spectral gain and the efficient energy conversion in active materials, organic semiconductor lasers are particularly useful for spectroscopic applications. They can cover the whole visible spectrum with only few active materials [21, 22]. Relying on distributed feedback (DFB) resonators, it allows the simple fabrication of laser devices with narrow bandwidth and low laser threshold, both being

favorable for Raman spectroscopy. Recently, organic semiconductor DFB lasers (DFB-OSL) have been applied for high resolution absorption and transmission spectroscopy [23–25]. As a promising candidate of excitation source for Raman spectroscopy, however, the DFB-OSL has to be improved through advanced fabrication techniques. In this contribution, we report Raman spectroscopy of sulfur (S_8) and cadmium sulfide (CdS) excited by DFB-OSLs. We show that these lasers can replace a bulky helium-neon (He-Ne) gas laser in Raman spectroscopy setup. The influence of the laser exciting power and laser spectral width was investigated.

2. Device design and characterization setup

There are some basic requirements on laser sources which must be met for Raman spectroscopy. These are adequate laser power, high wavelength stability, high spatial mode quality and moderately narrow line width [19]. To meet these criteria, we prepared a DFB-OSL with a high slope efficiency, a low divergence emission and a long-term stability. The organic semiconductor tris(8-hydroxyquinoline) aluminum (Alq_3) doped with the laser dye 4-(dicyanomethylene)-2-methyl-6-(*p*-dimethylaminostyryl)-4*H*-pyran (DCM) forms a very efficient and stable Foerster energy transfer system [26] and was chosen as the active gain material for our laser devices. To match the Alq_3 :DCM red emitter, we applied a glass grating (Visolas GmbH) with a one dimensional corrugation period of 400 nm as the second order distributed feedback resonator for a bottom emitting device. Compared to polymer substrates, the glass grating substrates have fewer fabrication defects and may avoid possible chemical reactions. The laser devices built on the glass gratings delivered higher slope efficiency, lower degradation rate and an improved beam profile. After the cleaning procedure, Alq_3 and 2.3% by weight of DCM were thermally co-evaporated in a high vacuum chamber with a thickness of 210 nm onto the glass grating substrate. An encapsulation was achieved by bonding a glass lid through ultraviolet curable optical adhesive (Norland, NOA68) [27, 28]. Figure 1(a) shows the encapsulated DFB-OSL when pumped on an area of $2 \times 10^{-3} \text{ cm}^2$ by a diode pumped passively Q-switched solid state laser (Crylas, FTSS355-Q2) with a wavelength of 355 nm. For a convenient coupling of the laser beam into the confocal microscope for Raman application, we utilized the bottom emission from device. The laser line width was investigated through measuring the full width at half maximum (FWHM) of the laser spectra at different pump pulse energies by a spectrometer (Acton, SpectraPro 300i, grating 1800 g/mm) connected to an intensified CCD-camera (Princeton Research, PiMax 512) at an optical resolution of 0.025 nm. As shown in Fig. 1(b), the FWHM of the laser spectra with the maximum at 629.3 nm grows from 0.11 nm to 0.26 nm, when the UV pump enhances from 60 nJ pulse^{-1} to $1.29 \text{ } \mu\text{J pulse}^{-1}$. This behavior is attributed to higher lateral modes which are excited for higher pump pulse levels [29]. The DFB-OSL exhibits a slope efficiency of 7.6% and a laser threshold of 28 nJ pulse^{-1} at a pump area of $540 \text{ } \mu\text{m} \times 425 \text{ } \mu\text{m}$ as shown in Fig. 1(c).

For Raman scattering measurements, the UV pump pulse energy was adjusted during the operation through a variable neutral density filter and controlled by a pulse energy meter (Coherent, LabMax-TOP). The maximal pump pulse energy could reach $3.2 \text{ } \mu\text{J pulse}^{-1}$. Under this pumping condition, our encapsulated organic semiconductor DFB laser achieved a maximal output pulse energy of $160 \text{ nJ pulse}^{-1}$, which corresponds to an averaged laser power of $780 \text{ } \mu\text{W}$ at a pump repetition rate of 10 kHz. The FWHM of the laser spectrum was measured as 0.50 nm.

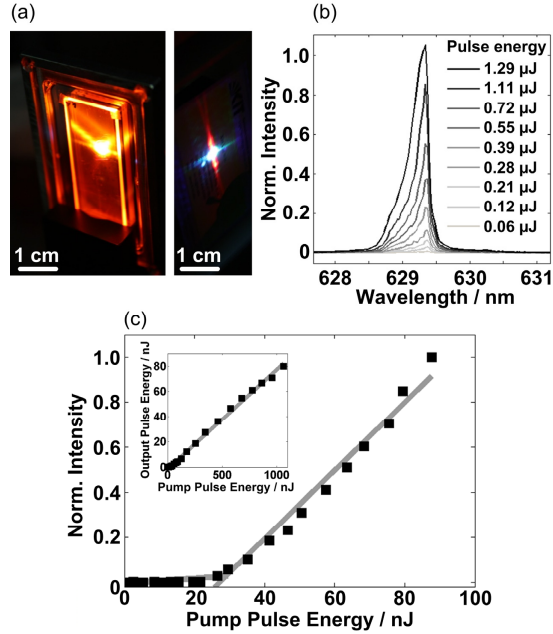


Fig. 1. (a) Photograph of an encapsulated DFB-OSL when pumped by the ultraviolet pump laser (left) and laser emission beam profile before coupling into the Raman measurement setup (right). (b) Laser spectra measured at different pump pulse energies. (c) Input-output characteristic at a wavelength of 629.3 nm for lower pump energy level and higher pump energy level (inset).

The Raman spectroscopy setup is shown in Fig. 2(a). It consists of a UV pump laser, the DFB-OSL, an inverted confocal microscope (Nikon, Eclipse TE2000-U) and a detection system. We inserted a clean-up bandpass filter (Semrock, F94-633L) with a bandwidth of 2.4 nm at the entrance of the confocal microscope to suppress ambient light and photoluminescence of the organic gain material. Making use of a 45°-tilted dichroic beam splitter (Semrock, F78-630), the organic laser emission is guided to excite the Raman scattering of the sample on a horizontal translation stage. Compared to more conventional laser, e.g., a He-Ne laser, the laser radiation of the DFB-OSL is emitted perpendicular to the substrate as a slightly divergent fan parallel to the orientation of the grating grooves as shown in Fig. 1(a). Applying a collimation lens and a 40 × objective with a numerical aperture of 0.6, the emitted laser stripe could be further focused to a length of less than 100 μm on the sample as shown in the inset of Fig. 2(a). The laser power on the sample was 350 μW. A longpass filter (Semrock, F76-633) was employed in the setup to further suppress the laser reflection and the Rayleigh scattering of the analytes. The collected Raman signals were analyzed and recorded by a spectrograph (Horiba, Triax 320, grating 300 g/mm) connected to a liquid-nitrogen-cooled CCD-Camera (Horiba, Symphony LN₂ detector). This combination of the detection system gave a spectral resolution of 0.26 nm, corresponding to a Raman shift resolution of 9.2 cm⁻¹ for our excitation wavelength at approximately 630 nm. At a temperature as low as 140 K, the dark counts of the CCD-camera were efficiently suppressed. The life time of the DFB-OSL is an issue in general and especially for Raman measurements requiring long integration times. We thus investigated the laser degradation characteristic through monitoring the excitation power while maintaining the pump pulse energy constant. As shown in Fig. 2(b), the laser emission from one pumped spot of the organic semiconductor laser decays only 10% within 30 min at a pump pulse energy of 3.2 μJ pulse⁻¹ and a high repetition rate of 10 kHz. This stability of one single pumped spot is sufficient to meet the demands of Raman spectroscopy.

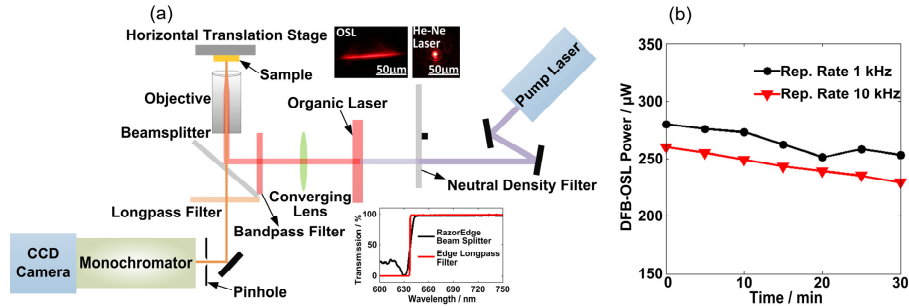


Fig. 2. (a) Scheme of the Raman spectroscopy setup. Inset top: Laser beam profiles of the DFB-OSL and the He-Ne laser at the position of sample. Inset below: The transmission spectra of the dichroic (RazorEdge) beam splitter and the longpass filter. (b) Degradation characteristics of the encapsulated Alq₃:DCM DFB laser under a pump pulse energy of 3.2 μJ pulse⁻¹.

3. Raman experiments and discussion

For the Raman experiments we applied sulfur as analyte. Sulfur (S₈) is a strong Raman scatterer with dominant bands at $\sim 219 \text{ cm}^{-1}$ and $\sim 473 \text{ cm}^{-1}$ [30, 31]. Currently, the Raman spectroscopy for sulfur and sulfocompounds attracts a lot of interest for in situ detection of marine organisms and minerals influenced by sulfidic environments [32–34]. Using an integration time of 50 s for spectra acquisition, we acquired Raman spectra of the sulfur sample (Sigma-Aldrich, >99.5%) excited by the DFB-OSL with an emission peaked at 629.3 nm. The Raman peaks at 219 cm^{-1} and 473 cm^{-1} can be easily identified from the recorded Raman spectra. With increased excitation power, the Raman signal intensity grew as well and was linearly proportional to the laser power as shown in Fig. 3(a). Above $120 \mu\text{W}$ excitation power the weak Raman band at 438 cm^{-1} can also be identified. Compared to the sulfur Raman spectrum excited by the He-Ne laser (Coherent, Model 200 single frequency stabilized HeNe laser) with a random polarization, we find a good correspondence in the Raman peaks at 219 cm^{-1} , 246 cm^{-1} , 438 cm^{-1} and 472 cm^{-1} . The polarization of the excitation source has no influence on the Raman lines of sulfur (S₈) due to the symmetry of the orthorhombic crystal [31]. As shown in Fig. 3(b), the width of the Raman lines is comparable with those excited by the He-Ne laser. The missing peaks at 154 cm^{-1} and 86 cm^{-1} in the excited Raman spectrum are explained by the filter function of the beam splitter and the longpass filter. The lower emission wavelength of the organic laser results in a small overlap of the attenuation range with Raman shifts smaller than 167 cm^{-1} as shown in Fig. 2(a).

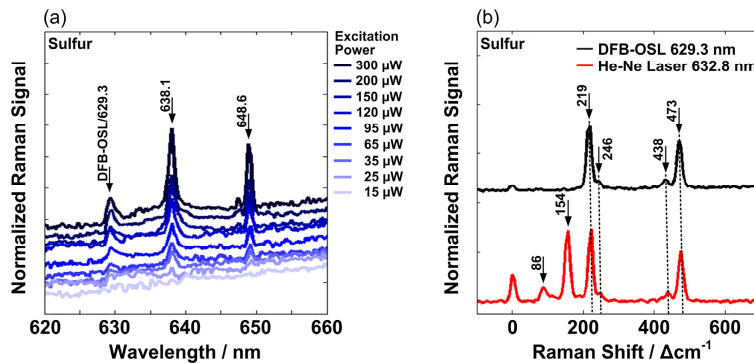


Fig. 3. (a) Raman spectra of sulfur (S₈) under varying excitation power of the DFB-OSL. (b) Comparison of the sulfur (S₈) Raman spectra excited by a DFB-OSL with a laser emission at 629.3 nm and by a He-Ne laser. (c) The growing signal intensity of Raman shift at 472 cm^{-1} with the increasing laser excitation power.

To realize wavelength tunability and to better match our optical filters we fabricated a continuously tunable DFB-OSL via evaporating a wedge-shaped active material layer onto the glass grating substrate. The fabrication details can be found in the work of S. Klinkhammer et al. [35]. Due to the correlation between the active layer thickness and the DFB-OSL emission wavelength, a specific organic laser emission wavelength can be obtained by pumping at a spatially defined position on the wedged layer. Figure 4(a) shows a photograph of the laser sample built on a glass grating substrate with a corrugation period of 400 nm after coating with a wedge-shaped film of Alq₃:DCM. It reveals a spatially rendering color which evolves from wedge-shaped thin films interference effects. The evaporated film thickness changes linearly from 190 nm to 380 nm as measured on a reference sample. We scanned the laser sample with a spatial resolution of 250 μm and a spectrum was taken at each point. The laser emissions vary from 617 nm to 653 nm continuously, as shown in Fig. 4(b).

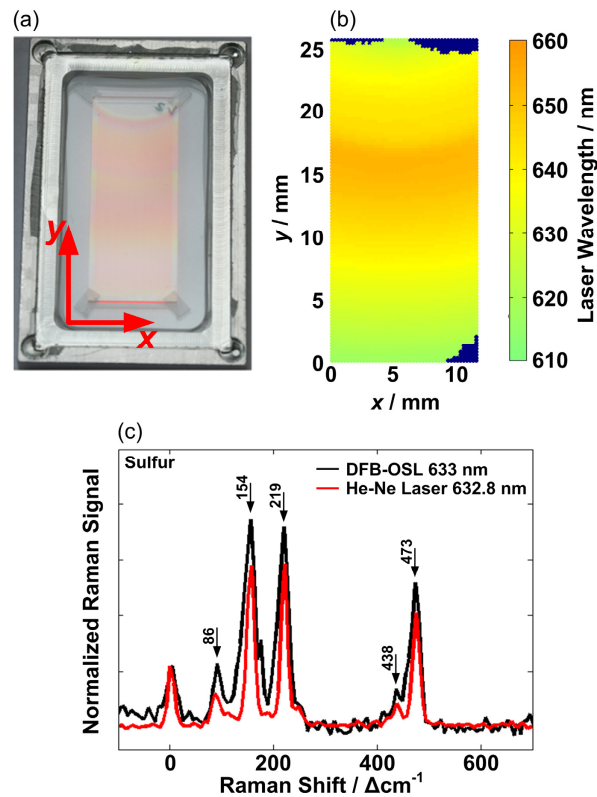


Fig. 4. (a) Photograph of an encapsulated spectrally tunable DFB-OSL with a continuously changing film thickness of Alq₃:DCM fabricated by rotating shadow mask evaporation. (b) Spatially resolved laser wavelengths of the laser sample. (c) Comparison of the sulfur (S₈) Raman spectra excited by the organic DFB laser with a laser wavelength of 633 nm and the He-Ne laser.

Using this approach we could tune our laser exactly to match the He-Ne laser wavelength and to optimally use the existing optical filters. For an integration time of 50 s the Raman peaks at 153 Δcm⁻¹ and 81 Δcm⁻¹ turned up and the Raman intensities are comparable with the ones excited by the He-Ne laser, as shown in Fig. 4(c). Only slight differences can be observed regarding the width of the Raman lines. Since the pump area on the organic laser sample (540 μm × 425 μm) for the tunable laser covered a slightly wedge-shaped organic layer, the laser line width grows to 0.62 nm for an UV excitation pulse energy of 3.2 μJ

pulse⁻¹. In turn, this leads to slightly broader lines than in case of excitation with the He-Ne laser.

We have also employed the DFB-OSLs to investigate the Raman spectra of other analytes. Figure 5 shows the Raman lines of cadmium sulfide (Crystal GmbH) excited by the non-wedged DFB-OSL with a laser emission at 629.3 nm. We can identify the two prominent Raman peaks at 307 Δcm^{-1} and 600 Δcm^{-1} , which originate from the CdS longitudinal optical (LO) phonon mode and the second longitudinal optical (2LO) phonon mode, respectively [36, 37]. In addition we could observe the other multiphonon scattering modes at 216 Δcm^{-1} , 249 Δcm^{-1} , 327 Δcm^{-1} and 346 Δcm^{-1} [38]. The Raman spectrum is comparable with the one excited by the He-Ne laser and corresponds well with the Raman database of the unoriented bulk wurtzite-type crystals of CdS [39].

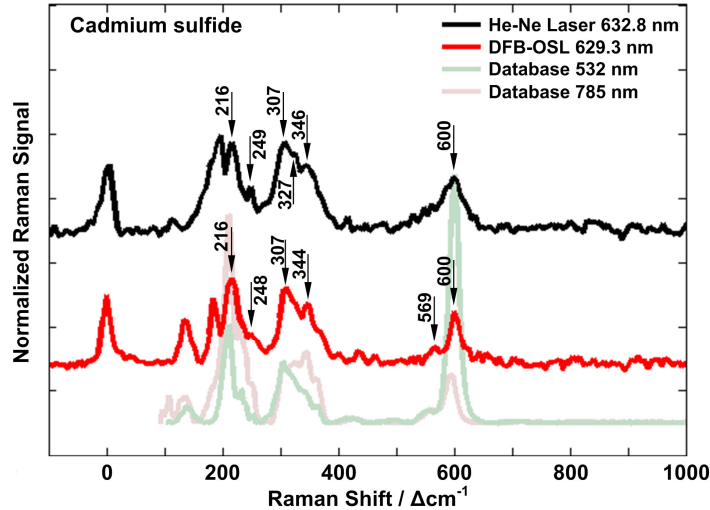


Fig. 5. Raman spectra of cadmium sulfide excited by the organic DFB laser with a laser wavelength of 629.3 nm and the He-Ne laser in comparison with the Raman database.

4. Conclusion

In conclusion, we have successfully applied organic semiconductor DFB lasers as excitation sources in Raman spectroscopy. Compared to the previous fabricated organic laser devices, our new lasers have been improved in terms of laser output efficiency, laser beam divergence and laser life time. Efficient laser excitation power up to 350 μW and a long-term stability were observed. The excited Raman spectra of sulfur and cadmium sulfide are demonstrated as examples. Our work paves the way to apply organic semiconductor DFB lasers in Raman spectroscopy. We foresee the advantages of organic lasers in resonance Raman spectroscopy and surface enhanced Raman spectroscopy due to their high tunability in visible spectrum range. Furthermore, the integration of organic lasers in lab-on-a-chip devices could enable the miniaturized Raman detection schemes for biomedical analysis.

Acknowledgments

The authors thank M. Hetterich and F. Maier-Flaig for supplying the Raman analytes, C. Kayser for technical assistance, K. Huska and S. Lebedkin for advices on confocal microscope, S. Klinkhammer and L.-M. Fleig for fruitful discussions. This work was supported by the Deutsche Forschungsgemeinschaft and the State of Baden-Württemberg through the DFG-Center for Functional Nanostructures (CFN). The work of X. L. is supported by Carl Zeiss Stiftung and Karlsruhe School of Optics and Photonics (KSOP). We acknowledge support by Deutsche Forschungsgemeinschaft and Open Access Publishing Fund of Karlsruhe Institute of Technology.